International Journal of Technology

http://ijtech.eng.ui.ac.id

Research Article

Immobilization Method of ZnO Nanoparticles on Nylon Monofilament Assembled as a Bottle Brush Model and Photocatalytic Activities on Rhodamine B Decomposition

Muhammad Adlim [1,2,*], Hana Abelia Putri [2], Alexandro Daffa [2], Kana Puspita[2], Ratu Fazlia Inda Rahmayani [1,2], Noor Hana Hanif Abu Bakar [3], Zul Ilham [4], Subhan Salaeh [5], Ismail Ozmen [6], Musa Yavuz [7]

[1]*Graduate School of Mathematics and Applied Science, Universitas Syiah Kuala, Darussalam Banda Aceh, 23111, Indonesia*
[2]*Chemistry Department, FKIP, Universitas Syiah Kuala, Darussalam Banda Aceh, 23111, Indonesia*
[3]*School of Chemical Sciences, Universiti Sains Malaysia, 11800 USM, Penang, Malaysia*
[4]*Institute of Biological Sciences, Faculty of Science, Universiti Malaya, 50603 Wilayah Persekutuan Kuala Lumpur, Malaysia*
[5]*Faculty of Science and Technology, Prince of Songkla University, Pattani campus, Pattani, 94000, Thailand*
[6]*Department of Chemistry, Faculty of Engineering and Nature Sciences, Suleyman Demirel University, Isparta, 32260, Turkey*
[7]*Department of Animal Science, Agriculture Faculty, Isparta University of Applied Sciences, Isparta, 32260, Turkey*
[*]*Corresponding author: adlim@usk.ac.id; Tel: 0651-7554229*

Abstract: Problems in light penetration, separation, reusability, and less adaptable reactors remain challenging in photocatalysis, especially when using slurry photocatalysts for wastewater decomposition. The immobilization technique of photocatalysts on compatible support and the reactor setup is crucial in achieving photocatalytic efficacy. This study aims to immobilize ZnO on nylon monofilaments from several precursors. The ZnO-coated nylon monofilament with appropriate characteristics is assembled as a "bottle brush model" catalyst support and integrated into a closed-flow photocatalytic reactor. The photocatalytic decomposition of rhodamine B (RhB) proved the efficacy of the new model catalyst support. The SEM images show the homogeneous surface of the ZnO-coated nylon monofilament, and the ZnO coating was stable in friction and water immersion. The ZnO coating was 44.967 μm; ZnO has aggregated particles, but most of the cluster size was less than 100 nm. The RhB (initial concentration of 5 ppm, 750 ml) photocatalytic activities (0.84 g of ZnO) reached up to 58% color reduction in 30 min, which is higher than the adsorption and photooxidation phenomena, which were only 20% and 13%, respectively. Based on the TOF comparison, the efficacy of this new model catalyst support with the rector design was higher than the activities of the slurry ZnO catalyst and others. The TOF is 0.09-0.30 mg of RhB per g of ZnO per minute, which is higher than the previously reported TOFs of most RhB slurry photocatalysis reported previously (0.003-0.05 $mg.g^{-1}.min^{-1}$). The present ZnO catalyst with the new model support is reusable twice, with ~ 10% of catalytic activity reduction.

This work was supported by Universitas Syiah Kuala WCU-ICR LPDP research funding, grant number 1/UN11.2.l/PT.01.03/PNBP/2024, 3rd May 2024, and The Bridging grant (304/PKIMIA/6316598) from Universiti Sains Malaysia partially funded this research.

https://doi.org/10.14716/ijtech.v16i5.7768
Received April 2025; Revised May 2025; Accepted June 2025

International Journal of Technology 16(5) 1772-1785 (2025)

Keywords: Photocatalytic decomposition; Polyurethane; Reactor; Rhodamine B; Turn over frequency

1. Introduction

Photocatalysts are used in several industries, including water treatment, air purification, hydrogen generation, CO_2 reduction, antimicrobial surfaces, organic synthesis, and solar cells. TiO_2 and Zinc oxide are popular photocatalysts with many applications (Madani et al., 2024; Silveira et al., 2022; Noman et al., 2021; Agustina et al., 2020; Yudha et al., 2020; Hudaya et al., 2018; Sharfan et al., 2018). ZnO is a prominent photocatalyst because it has antimicrobial properties, high electron mobility, and is a relatively environmentally friendly and stable compound (Hanh et al., 2024; Look, 2001). Usually, ZnO is a slurry photocatalyst (Alzahrani et al., 2023; Muktaridha et al., 2022; Nguyen and Nguyen, 2020) with some problems. The slurry catalyst usually uses ZnO as powders or ZnO supported in fine solid particles, but it still blocks light penetration and is not easily scaled up. Therefore, the novel immobilizing method will be a crucial study. Moreover, most known ZnO preparation involves high-temperature annealing, which requires a heat-resistant material support. Recently, studies on low-temperature ZnO preparation have been introduced (Hidayat at al., 2023; Wahid et al., 2023; Supin et al, 2023; Edalati et al., 2016), inspiring the immobilization of ZnO from the precursor on nylon fiber or monofilament, as the focus of this current study.

Cost-effectiveness is crucial in industrial applications; this study compares three ZnO precursors with different production costs. The precursors are ZnO powder (ZnO-P), which is much cheaper. Commercial nanoparticle ZnO (ZnO-NC) is prepared by grinding (top-down approach), and a synthetic nanoparticle ZnO (ZnO-NS) is made from the salt precursor (bottom-up approach). This study focuses on immobilizing ZnO from the precursors on nylon monofilament with compatible techniques to obtain a stable coating. A bottle-brush model was used to construct the ZnO-coated monofilament. This new model is introduced in this photocatalyst preparation. ZnO was immobilized on flat glass, fiberglass, and fiberglass cloth installed on several types of reactors; classical annular, tube light, fluidized bed, spinning disk, optical fiber, LED, micro, integrated membrane, capillary array, and pack are among the existing photocatalytic reactors bed (Fallahizadeh et al., 2024; 2023; Bhatti et al., 2023; Humayoun et al., 2023; Li et al., 2023; Le et al., 2022), but all are different from this bottle brush model integrated with a closed flow reactor system. Unlike in a slurry system, ZnO immobilized at bottle-brush model support hypothetically gives a higher surface area, light penetrates better, the catalyst is easily separated, and it can be easily reused. The activity of synthetic ZnO photocatalysts with and without doping is usually monitored from the decomposition of rhodamine B (RhB) solution, verifying several photocatalytic studies (Muktaridha et al., 2023). RhB is a non-biodegradable and organic chlorinated salt that has relatively high toxicity (Hanh et al, 2024). The ZnO immobilization technique on nylon monofilament is still challenging because ZnO does not easily attach and is less stable within a moving liquid. Therefore, this research aims to study a new immobilization method named the bottle brush model with cost-effective materials, which hypothetically has high photocatalytic activities, easy separation between catalyst and substrate, easy scale-up, and activities comparable to those of the existing slurry methods.

2. Methods

Several materials were used in this research, including polyurethane (PU) adhesive and monofilament nylon (∅ 0.9 mm). All chemicals with reagent or PA grades were obtained from Sigma-Aldrich or Merck Germany. Chitosan (MW of approximately 400,000) was purchased from Sigma-Aldrich in Germany. The other chemicals used were zinc oxide (ZnO commercial, ACS Reagent), zinc nitrate hexahydrate crystal ($Zn(NO_3)_2.6H_2O$; 98%, reagent Grade, Merck), ZnO commercial nanoparticles (<100 nm; Merck), rhodamine B ($C_{28}H_{31}ClN_2O_3$, Merck), distilled water, steel wire (∅ 1 mm), Tinner, methanol (≥ 99%, Merck), NaOH (≥ 97%, Merck).

A new design photocatalytic reactor system is equipped with 6 units of @8-watt UV lamps (total light intensity of 123.4 lx, λ = 360 nm), a delay relay timer, a stopwatch, and two mini 12 V DC water pumps. Some of the analytical instruments used were a UV-Vis Shimadzu 1800, an Absorption Spectrometer (iCE 3000 Series, USA), a scanning electron microscope (JEOL JSM 6360 LA, Japan), and an X-ray diffraction (XRD) Shimadzu 7000. Sample images and particle size were observed using a binocular microscope (Olympus SZ61, Japan) with a camera (Optilab, China) and a transmission electron microscope (JEOL JEM-1400, Japan). The entire research work is illustrated in Figure 1.

2.1. Synthesis and Characterization of ZnO NPs

ZnO from different precursors is denoted as ZnO powder (ZnO-P), ZnO nano commercial (ZnO-NC), and ZnO nano synthesis (ZnO-NS). ZnO-P and ZnO-NC were used directly without further treatment. ZnO-NS was prepared as follows: a chitosan solution was prepared by modifying a previous report (Hidayat et al., 2023). $Zn(OH)_2$ was precipitated by adding aqueous methanol NaOH to a chitosan matrix. The residue was centrifuged at 4000 rpm before being filtered and heated at 70°C for 72 h, verifying the low-temperature preparation (Hidayat et al., 2023; Edalati et al., 2016).

2.2. Immobilization of ZnO on nylon monofilament, characterization, and stabilization test

Each type of ZnO was ground and sifted through a 120 mesh sifter and immobilized on nylon monofilament. Two adhesives were tested: polyurethane and expanded polystyrene. The nylon monofilament was vertically hung and tied with a 200-g plumb bob to straighten and stretch. The nylon monofilament was passed through an extruder filled with adhesive, and then the nylon was coated with adhesive before passing through the ZnO flask. ZnO particles will stick to the nylon-coated adhesive with pressure. ZnO immobilized on the nylon monofilaments was air-dried for 24 h. ZnO-immobilized filaments were dried and weighed until they reached a constant weight. The coating was soaked in 100 mL of distilled water and rotated in a rotary evaporator at 40 rpm for 10 min to test the coating stability (Hidayat et al., 2023). The weight difference of ZnO before and after spinning within the rotary evaporator was deduced as the ZnO stability on the filament. The Zn content was analyzed using the AAS method; the surface was observed using SEM and a light microscope, and FT-IR monitored possible chemical interactions between adhesives and ZnO. ZnO-coated nylon monofilament (ZnO-CNMF) was assembled with stainless steel wires by inserting and twisting two steel wires until it looked like a bottle brush with unit dimensions of 10 cm in length and 4 cm in diameter.

2.3. Photocatalytic reactor setup, photocatalytic degradation, and optimum contact times

A detailed description of the new photocatalytic reactor is provided in the Results and Discussion section. The photocatalytic reactor was filled with 500 mL of 5 ppm (5 mg/L) RhB (250 mL in the container and 250 mL in the reservoir). Four bunches of ZnO-immobilized monofilament with bottle brush model support (immobilized ZnO; with 0.3600 g of ZnO content) were installed in the photocatalytic reactor. The time-relay was set at 5 min for running and 5 min for waiting cycles. The UV lights (6 units @8-watt with a total light intensity of 123.4 lx, λ = 360 nm) and 6 computer fans were turned on, and every 5 min of running, RhB was sampled, and the percent RhB degradation was counted based on the absorbance comparison (Alshehri et al., 2024). During photocatalysis, the casing was used to cover the reactor to avoid external light interference. The samplings lasted up to 120 min to determine the optimum contact time, and the absorbance was compared with control-1 (without light or in the dark) and control-2 (without catalyst with light on).

Photocatalysis was repeated at the optimum contact time with various amounts of immobilized ZnO catalyst. The experiment was repeated on a constant amount of catalyst (0.657 g of ZnO, 6 bunches) and tested with various RhB concentrations (2, 3, 4, 5, and 6 mg/L). Experiments were

compared among different sources of ZnO: ZnO-P, ZnO-NC, and synthetic ZnO-NS. The temperature was monitored and maintained by 5 computer fans installed in the reactor.

In the ZnO-P reusability experiment, the used ZnO-P was washed with water-ethanol (1:1) several times and air-dried until it reached a constant weight. ZnO-P was installed in the reactor and used for RhB photocatalysis. The RhB solution was periodically sampled. A similar procedure was repeated for the next reusability test.

2.4. Kinetic studies

Irradiation of RhB with UV light can cause photo-oxidation, adsorption, and photocatalysis. Several sets of experiments were set up to identify the dominant. Photooxidation was studied by irradiating RhB without a catalyst. The adsorption phenomenon was followed by comparing the change in RhB absorbance for each individual and a combination of ZnO, PU adhesive, and chitosan. The kinetics study will follow a model of photocatalytic degradation in a water medium. The Langmuir–Hinshelwood model can then be plotted, verifying that photocatalytic decomposition follows the first-order reaction (Ghasemi et al., 2016). The catalytic activity was directly monitored from the reaction rate compared to the control. The amount of product or reactant change per catalyst weight per period is considered the catalyst efficiency or turnover frequency (TOF) (Basumatary et al., 2024).

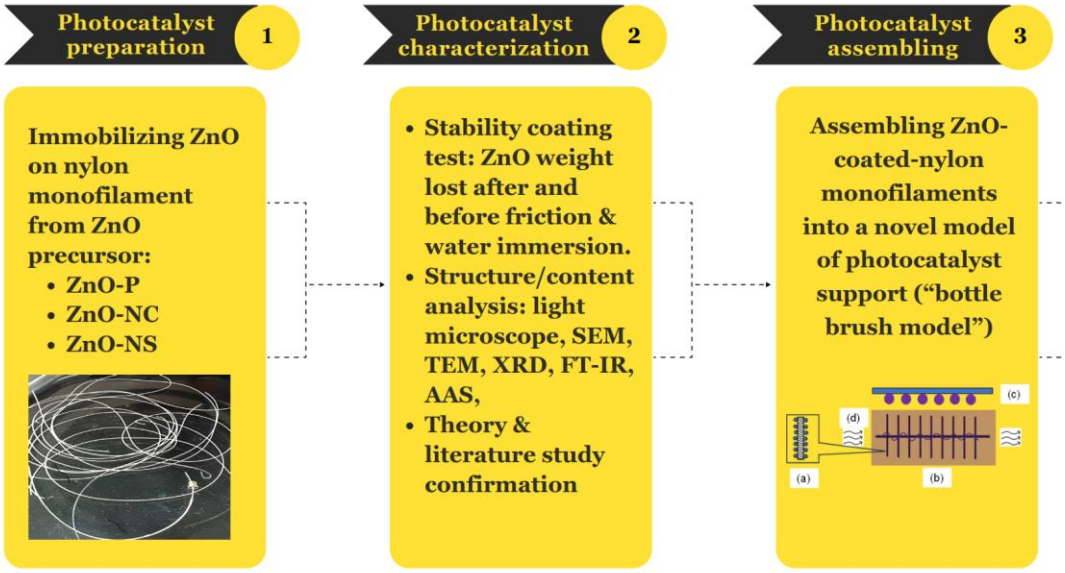

Figure 1 Flow chart of the research methodology used

3. Results and Discussion

3.1. Synthetic and commercial ZnO properties of chitosan

ZnO-P and ZnO-NC were purchased from a chemical supplier (Sigma) as powder and nanopowder, respectively. ZnO-NS was synthesized using the hydrothermal method in methanol-acetic acid (1:1) at low-temperature heating, which verified the previous low-temperature procedures involving chitosan as the stabilizer (Hidayat et al., 2024; 2023; Muktaridha et al., 2022). ZnO-NS is active in UV radiation (Nafees et al., 2013) since the preparation is similar to the previous method, where the bandgap must not be much different from 3.48 eV (Aouadi et al., 2024) or 3.2 eV (Muktaridha et al., 2022).

Each type of ZnO was analyzed with XRD, and all ZnO catalysts showed similar diffractogram patterns. ZnO-P and ZnO-NC have higher crystallinity than ZnO-NS, which contains chitosan (in supplement material-Figure 1). Chitosan, which has amorphous plasticity characteristics, covered the ZnO particles.

3.2. Stability of immobilization

Each ZnO-coated monofilament was stable in water and during friction. Approximately 1% of the ZnO weight was lost due to friction in the rotary evaporator test. The mean weights of ZnO-P, ZnO-NC, and ZnO-NS stuck on monofilament nylon were 0.001, 0.001, and 0.0003 g per cm, respectively.

3.3. Characterization of the ZnO coating on the nylon monofilament

Nylon monofilament is an inert and colorless material; however, after coating with PU and ZnO, it turned white due to the ZnO coating (see Supplementary Material Figure 2a). Coating thickness testing was performed by cutting the cross-section of the ZnO-coated nylon monofilament and observing it using a light microscope to measure the diameter. The monofilament diameter was 989.421 μm, and the coating thickness was nearly similar for each ZnO type with a mean of 45.57± 2 μm, as represented by the images (Figure 2b in the Supplementary Material).

The ZnO homogeneity coating on the monofilament was studied using scanning electron microscopy (SEM) images (Figure 3). At a 100x magnification, ZnO-P showed dense particles, and the ZnO-NC has a homogenous and smoothest surface. The ZnO-NS was not a fine particle because it contains flake-shaped dried chitosan. At 30,000x enlargement, the ZnO-P particles appeared as particulates, while the ZnO-NC particles appeared crystalline and the ZnO-NP particles were cluster flakes. The adhesive did not fully cover the entire ZnO particle surface; therefore, ZnO was still assessable as a reactant (see Supplementary Material Figure 3).

The particle size of ZnO on the nylon monofilament was studied using the high-performance transmission electron microscopy method. The particles were aggregated, rod-shaped, possibly hexagonal, smaller than 200 nm, and many < 100 nm in size (in supplement material- Figure 4). ZnO-NS particles appear to be much smaller but are packed in a chitosan film (in the supplement material, Figure 5c). The morphology confirms that some particles have crystalline shapes with a relatively large particle size deviation. Although ZnO-P was a commercial bulk particle, some were nano-sized.

Nylon monofilament is an inert and strong polyamide polymer that is usually used as a fishing line (Thomad and John, 2009). The only possible chemical interaction between PU adhesive and ZnO representative (ZnO-P) was studied by comparing the FTIR data of PU, ZnO-P, and PU-ZnO-P. Some bands represent both PU and ZnO. The bands were recorded at 3416 cm^{-1} (secondary amine, =N-H), 2875 cm^{-1} (N-H), 2275 cm^{-1} (isocyanate -N=C=O), 1660 cm^{-1} (-C=O), which are all PU functional groups, and 831 cm^{-1} (Zn-O) is from ZnO (in supplement material-Figure 5a) (https://instanano.com/all/characterization/ftir/ftir-functional-group-search/). Bands at 3367, 1660, and 2875 cm^{-1} represent chitosan functional groups of O-H, N-H, also existing in ZnO-NS. The FTIR spectra verified the previous report of the ZnO-chitosan composite (Medany et al., 2024).

3.4. New design and setup of rector photocatalysis

Based on the literature, the newly developed reactor in the current study differs from the known photocatalytic reactors (Abdel-Maksoud et al., 2016). The design was a modification from our previous report, in which ZnO was immobilized on a flat-surface fiberglass cloth installed in a loop bath photocatalytic reactor (Muktaridha et al., 2022).

The ZnO-coated nylon monofilament with PU as the adhesive gave ZnO efficient use. Hypothetically, the ZnO particles on the monofilament were less dense, had a better particle distribution, and therefore had a higher surface area, making the ZnO surface more accessible to the reactant (Figure 1A) than the ZnO coated on a flat surface, such as cloth and glass slides.

The SEM image (in Supplementary Material, Figure 3) shows that ZnO particles attached strongly to the nylon monofilament and were stable without significant loss of weight, as deduced from the friction test and water immersion data. The stickiness of the ZnO particles on the monofilament surface is illustrated in Figure 2Aa. The ZnO-coated monofilaments were assembled as a bottle brush model (Figure 2Ab). Small exhaust fans were installed in the experiment to eliminate the effect of UV heat on the studies (Figure 2Ad). In industrial applications, the nylon

monofilament can be replaced with cable ties attached to PVC pipes (Figures 6a and 6b in the Supplementary Material). This removable photocatalyst was easier to adjust and maintain. Unlike most photocatalytic reactors (Muktaridha et al., 2022; Jesitha et al., 2021), light can penetrate the reactant solution effectively (Figure 2B). The adjustable water circulations were controlled with a time relay for the speed and contact time. This system caused the photocatalyst to have higher efficacy than the stirring method. Stirring with fast fluid flow can block light penetration and damage the photocatalyst. The UV in a vertical and adjustable position (Figure 2B) can also imitate sunlight irradiation in industrial applications (in supplement material-Figure 6b).

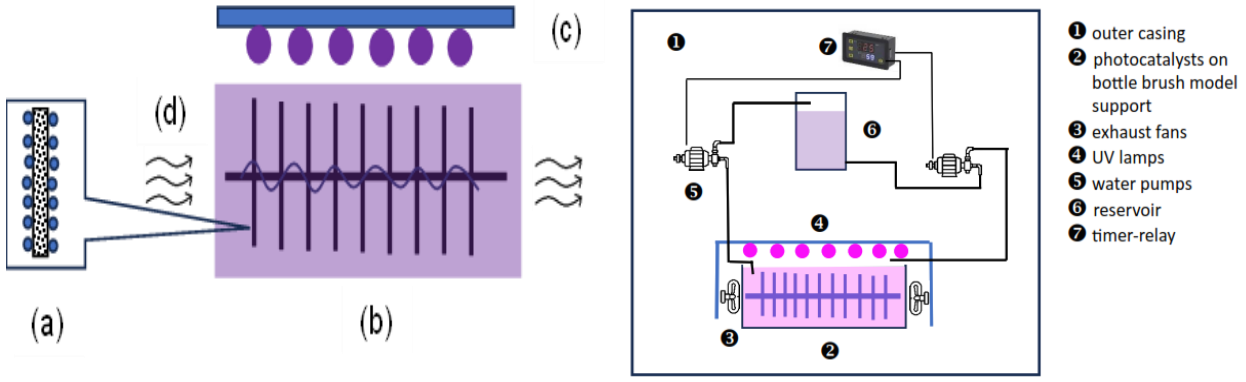

(a) (b)

Figure 2 (a) ZnO-coated monofilament assembled as a bottle brush model support. (b) New adjustable photocatalytic reactor

3.5. Efficacy of the New Photocatalysis Design

The photocatalyst's efficacy was measured from RhB color degradation, as a known substrate model for photocatalytic studies, verifying the literature (Lal et al., 2023; Muktaridha et al., 2023). UV-Vis spectrophotometry could be a combination of photo-oxidation, which is usually a slow reaction, adsorption (the RhB color was absorbed by catalyst material), and photocatalytic degradation (RhB degraded to colorless molecules of CO_2 and H_2O, NH_4^+, NO_3^-), which is well known in the literature (Natarajan et al., 2011; He et al., 2009).

As shown in Figure 3(a), the optimum contact time between RhB and the supported ZnO (0.3600 g of ZnO content) photocatalyst was 50 min for all ZnO types. RhB absorbance decreased up to 75% and remained constant after 50 min. After 50 min, the absorbance reduction slowed.

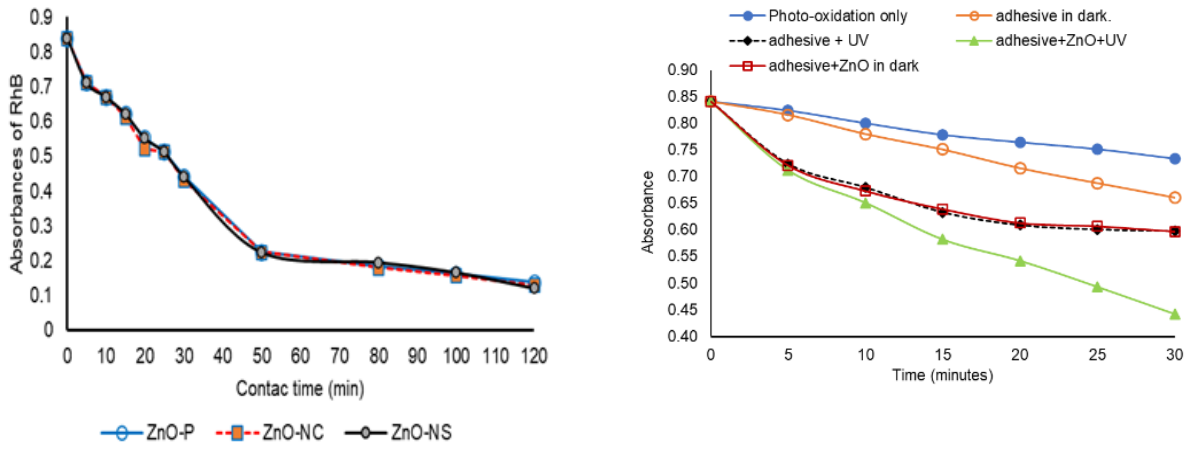

(a) (b)

Figure 3 (a) Optimum contract time at 0.3600 g of ZnO, (b) absorbance degradation in each experiment of ZnO-P at a constant concentration (0.3600 g)

3.5.1. Photooxidation of RhB

The interaction of light with RhB over a long irradiation period can cause color fading, known as the photo-oxidation effect (Sabatini et al., 2018). Photo-oxidation, adsorption, and photodegradation cause RhB color degradation. Control experiments were performed under uniform conditions and normal pH to differentiate them (Figure 4b). The photo-oxidation effect, represented as PO (Figure 4a), was studied by irradiating RhB with UV (UV only) without the ZnO catalyst composite. By which only photo-oxidation factor and not possible absorption and photocatalysis could occur. This contributed approximately 13% of the RhB absorbance reduction in 30 min and was the slowest reaction compared to adsorption and photocatalytic degradation, as shown in Figure 3(b). Photo-oxidation occurs when UV irradiation penetrates the RhB solution and makes RhB fade. This is due to the characteristic properties of RhB photosensitization (Sayem et al., 2024). UV oxidizes the water molecules and forms a small amount of peroxide (H_2O_2), which bleaches RhB; then, RhB fades slightly, as indicated by the decline in absorbance. The H_2O_2 might attack the RhB chromophore site without ZnO. It was a slow reaction (13% of [RhB] in 30 min) and was theoretically known (Thao et al., 2017) compared to adsorption and photocatalytic phenomena.

3.5.2. Adsorption

The experiment was conducted in the dark (dark + glue) in which PU-coated monofilament was immersed in RhB solution to explore the glue absorption effect on RhB solution, denoted as ABS (Figure 4a). The combination of PO and ABS with and without ZnO (marked as POABS1 and POABS2 in Figure 4a) was lower than the photocatalytic degradation of PCD (Figure 4a). Since there was no light, photo-oxidation and photocatalysis did not occur. The combination of PO and the adsorption effect caused a reduction in the mean RhB absorbance of 13.3%. Absorption occurred when the monofilament was coated with a thin layer of polyurethane adhesive. Although the coating thickness was only 44.967 μm, the RhB aqueous solution was trapped within its foam pores (Sudol and Kozikowska, 2021).

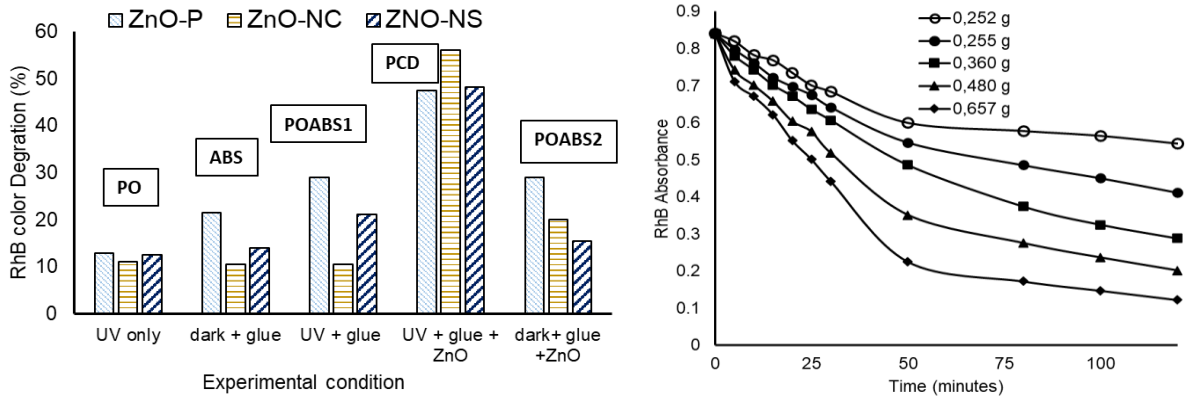

(a) (b)

Figure 4 (a) Several possible effects on the photocatalytic decomposition of RhB after 30 min of contact times at relatively similar amounts of catalyst; PO = photo-oxidation; ABS = absorption; POABS1 = PO + ABS without ZnO; PCD = photodegradation; POABS2 = PO + ABS + ZnO. (b) Representative curve showing the effect of the amount of ZnO-P on RhB degradation

3.5.3. Photocatalytic degradation

The reaction rate was much higher in photocatalytic degradation (designated as PDC in Figure 4a) when ZnO was present and UV irradiation was on. The reaction rate was measured from the RhB color degradation, which is known as the decoloration efficiency. The photocatalytic degradation is much higher than the photo-oxidation and absorption phenomena. The photocatalytic activities of all ZnO types were nearly similar which was 50-58% in 30 min, as shown

in Figure 4a, but the amount of catalyst involved was different. The amount of ZnO involved in the reaction was 0.66 g of ZnO-P in 500 mL of 5 ppm RhB, 0.84 g of ZnO-NC in 750 mL of 5 ppm RhB, and 0.21 g of ZnO-NS in 750 mL of 5 ppm RhB. The amount of catalyst affected the RhB color degradation as a representative graph shown in Figure 4b, by which the kinetics can be calculated.

Each experiment used 6 catalyst bunches with a total weight of ZnO-P (0.66 g), ZnO-NC (0.84 g), and ZnO-NS (0.21 g). ZnO-NS is less stuck on the monofilament compared to ZnO from other precursors. The plasticity properties of chitosan prevent the chitosan film from forming fine particulates. However, ZnO-NS showed the highest photocatalytic efficacy based on the TOF. Because the preparation of ZnO-NC and ZnO-NS was expensive and involved complex procedures, ZnO-P is an acceptable photocatalyst because it is much cheaper and has comparable photocatalytic activities. The price comparisons are US$ 67 per 10 g (ZnO-NC, nanopowder, size < 100 nm), US$ 82 per 500 g (ZnO-P, ACS, Reagent.), US$ 120 per 500 g (ZnO precursor: $Zn(NO_3).6H_2O$, reagent grade, 98%), and US$ 128.7 for 50 g (chitosan, medium MW) (https://www.sigmaaldrich.com/).

In photocatalytic degradation, the RhB molecule is broken down into smaller colorless molecules known as mineralization. The interaction of UV, ZnO, and RhB can be explained using photochemistry theory. UV, which has a wavelength of 100-400 nm, emits photons (hν, $\lambda \leq 380$ nm), causing excited electrons within the ZnO lattice and producing e^- and positive hole (h+) pair at the conduction band (e_{CB}^-) and the valence bond (h_{VB}^+). The e_{CB}^- interacts with O_2 to produce superoxide (Lal et al., 2023). The radicals reproduce in cycles, and some attack the RhB molecules to induce mineralization, which breaks the molecules into smaller fragments and finally produces colorless molecules (CO_2 and H_2O), NH_4^+, and NO_3^- as indicated by RhB absorbance reduction (Wang et al., 2018). The mechanism has been previously reported and verified in many journals (Hanh et al., 2024; Sayem et al., 2024; Rajendrachari et al., 2021). This study also confirmed the existence of NH_4^+ with Nessler reagent.

The radicals are reactive oxygen species (ROS), and their role in photodegradation is already known (Sayem et al., 2024). ROS is an unstable molecule with an extremely short lifetime, and it tends to stabilize quickly by binding with other radicals, unpaired-electron molecules, or scavenger materials (Zhang et al., 2023). Therefore, after attacking RhB molecules, ROS bind to other radicals and form stable molecules, as is known in the concept of the radical chain reaction. Hypothetically, when the amount of RhB is not less than that of ZnO, the excess ROS might change into stable molecules (R••R). In reality, wastewater samples might contain other substances, such as proteins (bigger molecules than RhB) and minerals, which are less reactive than ROS, but have been reported as ROS scavengers (Joorabloo and Liu, 2024). The ROS mechanism in photodegradation has been proposed in the literature (Hanh et al., 2024; Sayem et al., 2024; Rajendrachari et al., 2021).

The effect of the amount of ZnO photocatalyst on the rate of photocatalytic RhB decomposition was studied under consistent experimental conditions. Still, at various amounts of photocatalyst (Figure 4b) shows the amount of each ZnO catalyst that affects the amount of RhB decomposition with a linearity of 0.9-0.99, which means the photocatalytic degradation was not a zero-order reaction, which confirms the Langmuir–Hinshelwood (L-H) model that photocatalysis is a pseudo-first-order reaction (Ghasemi et al., 2021). The rate expression of L-H model : $r = \frac{kKC}{(1+KC)}$ and at a low reaction concentration of first-order kinetics, r = kKC and $r = k_{app}C$; $k_{app} = k_{cat}K$. Linearize the L-H equation, and give $\frac{1}{r} = \frac{1}{kKC} + \frac{1}{k}$, the plot of this equation is shown in Figure 4, which cites a previous report (Ollis, 2018).

K_{app}(s^{-1}), k_{cat}(mol. $L^{-1}.s^{-1}$), and K($L.mol^{-1}$) can be obtained as the reciprocal slope and intercept of Figure 5(d-f), which are (0.013; 0.060; 0.216), (0.010; 0.034; 0.288), and (0.012; 0.040; 0.302) for ZnO-P, ZnO-NC, and ZnO-NS photocatalysis, respectively. The rate constant (k_{cat}) is larger in ZnO-P (0.06 mol. $L^{-1}.s^{-1}$) photocatalysis than in ZnO-NS (0.040 mol. $L^{-1}.s^{-1}$) reaction, but ZnO-NS

photocatalysis used a much lower amount of catalyst, which was 30% of ZnO-P weight (Figure 5a-c).

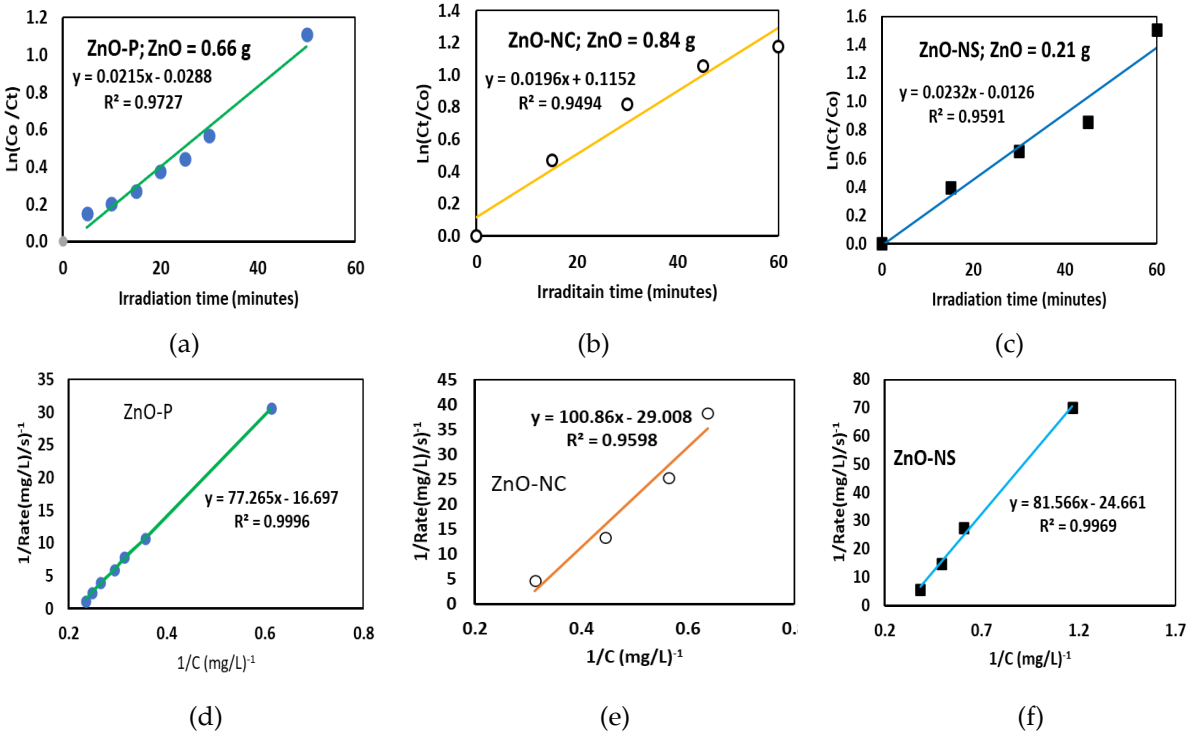

Figure 5 Kinetics of RhB degradation catalyzed by (a) ZnO-P, (b) ZnO-NC, and (c) ZnO-NS. The reciprocal initial rate is plotted against the reciprocal concentration of RhB catalyzed by (d) ZnO-P, (e) ZnO-NC, and (d) ZnO-NS

3.6. Comparison of the TOF of ZnO immobilized on nylon monofilament with previous reports

The photocatalytic properties of various types of ZnO immobilized on nylon monofilament are higher than those of other research findings, as shown in Table 1. Previous studies have shown a higher percentage of RhB discoloration (Lal et al., 2023). However, the RhB volumes were much smaller; a higher amount of ZnO and stronger UV light were used. The experimental conditions were different. However, by calculating the TOF, the catalyst performances are comparable.

Unlike ZnO immobilized on fiberglass cloth (Muktaridha et al., 2023), ZnO immobilized in nylon monofilament provides a larger surface area interaction with fewer catalysts, as indicated by the TOFs. In slurry conditions, the solution thickness affects the light penetration; therefore, these can only be applied in small volumes. Catalyst separation is required, and catalyst reusability is almost impossible. This limitation was overcome by immobilizing the photocatalyst in nylon monofilaments and assembling them as a brush bottle support, as established in this study.

The efficacy of the current ZnO catalysts (ZnO-P, ZnO-NC, and ZnO-NS) is high, with TOF values of 0.06, 0.09, and 0.3 mg RhB per gram of catalyst per minute. The high catalytic activity of ZnO-NS might be correlated with the use of chitosan as the stabilizer. The amino groups of chitosan provide lone pair electrons to host Zn^{2+} by making coordination bonds with zinc ions (Yazdani et al., 2017) and dispersed thoroughly within the chitosan matrix before it was oxidized into ZnO. Therefore, chitosan prevents ZnO from agglomerating into larger particles (in supplement material-Figure 4), keeping it in nano size, resulting in a larger surface area. Chitosan within ZnO-NS absorbed RhB (Pompeu et al., 2022) and brought it closer to ZnO, causing ZnO to effectively attack the RhB molecules to decompose, resulting in the highest TOF.

ZnO-P was prepared directly from ZnO powder, and ZnO-P has the lowest TOF compared to the others, as shown in the series of ZnO-P < ZnO-NC < ZnO-NS. However, ZnO-P is cost-effective

because it can be used from commercially available powder, is cheap, and requires no further laboratory preparation. ZnO-NC was prepared from commercial ZnO nanoparticles, which are expensive. ZnO-NS preparation is considered a high-cost and complicated synthesis.

The used ZnO-P was reusable at least twice because the catalytic activities slightly decreased (only 10%) compared with the fresh ZnO-P (in the supplement material, Figure 7).

Table 1 Performance comparison of ZnO-catalyzed immobilized nylon monofilament with other studies

ZnO preparation	ZnO Support	UV (Watts)	Kinetics (Pseudo 1st order)	TOFs ($mg.g^{-1}.min^{-1}$)	Reference
Synthetic nanoparticles	Fiberglass cloth	48	$k = 41 \times 10^{-4}$ min^{-1}	0.003	(Muktaridha et al., 2023)
Commercial (ZnO-P)	Brush bottle model*	48	$k = 0.021$ min^{-1}	0.060	This study
Commercial Nanopowder (ZnO-NC)	Brush bottle model*	48	$k = 0.020$ min^{-1}	0.090	This study
Synthesis nanoparticles (ZnO-NS)	Brush bottle model*	48	$k = 0.020$ min^{-1}	0.300	This study
Synthetic nanoparticles,	No support, Slurry	22	k = not available	0.050	(Piras et al., 2022)
Synthetic nanoparticles	No support, Slurry	216	k = not available	0.020	Lai et al., 2023
Nanopowder	No support, Slurry	125	k = not available	0.040	Nagaraja et al, 2012

*Immobilized on nylon monofilament and assembled as a brush-bottle model

4. Conclusions

This study proved that several types of ZnO can be successfully immobilized on nylon monofilament using polyurethane (PU) as the adhesive. The ZnO-coated nylon monofilament was stable in friction with insignificant weight loss of ZnO during several hours of water immersion. The ZnO-PU has mean dimensions of 982.554 µm in diameter and a thickness of 62.077 µm. ZnO particle aggregation was < 200 nm and most were <100 nm. ZnO-immobilized on nylon monofilament assembled as bottle-brush model-support catalytically decomposed rhodamine B (5 ppm) solution with efficacy up to 50-58% decoloration in 30 minutes using 0.21-0.8 g of ZnO under UV light. ZnO particles immobilized on nylon monofilament with brush bottle model support and installed in a closed-flow photocatalytic reactor confirmed higher photocatalytic activity than previously reported studies based on the TOF comparison. It is more cost-effective than other ZnO precursors. The photocatalytic efficacy of the slurry prepared by this method is higher than that of a slurry and flat support photocatalysis. This model catalyst support and reactor can be scaled up and adapted to a sunlight system, and the catalyst can be reused at least twice. These findings solve the problem of light penetration blockage, the separation of catalyst-reactant difficulty in photocatalysis. So far, the catalytic application is limited to UV, and most is still laboratory scale; however, photocatalysis can be applied on an industrial scale with relatively low cost using this model (bottle-brush supported ZnO photocatalyst) integrated with the new reactor design, which is easily adjustable under sunlight. In a real sample, the transparency and chemical content of wastewater might affect the catalyst activity. Although excessive ROS can be easily stabilized, it has not been confirmed.

Acknowledgements

This work was supported by Universitas Syiah Kuala WCU-ICR LPDP research funding with grant number 1/UN11.2.l/PT.01.03/PNBP/2024, 3rd May 2024. The Bridging grant (304/PKIMIA/6316598) from Universiti Sains Malaysia partially funded this research.

Author Contributions

Research ideas and design (Muhammad Adlim), laboratory works (Hana Abelia Putri, Alexandro Daffa 2), lab supervision (Kana Puspita, Ratu Fazlia Inda Rahmayani), typical sample characterization (Noor Hana Hanif Abu Bakar), publication guidance & proofread (Zul Ilham, Subhan Salaeh, Ismail Ozmen, Musa Yavuz).

Conflict of Interest

The authors declare that they have no known competing financial interests or personal relationships that could have appeared to influence the work reported in this paper.

References

Abdel-Maksoud, Y, Imam, E & Ramadan A 2016, 'TiO_2 solar photocatalytic reactor systems: selection of reactor design for scale-up and commercialization analytical review', *Catalysts*, vol. 6, article 138, https://doi.org/10.3390/catal6090138

Agustina, TE, Melwita, E, Bahrin, D, Gayatri, R & Purwaningtyas, IF 2020, 'Synthesis of nano-photocatalyst ZnO–natural zeolite to degrade Procion Red', *International Journal of Technology*, vol. 11, no. 3, pp. 472–481, https://doi.org/10.14716/ijtech.v11i3.3800

Alshehri, A, Alharbi, L, Wani, AA & Malik, MA 2024, 'Biogenic *Punica granatum* flower extract assisted $ZnFe_2O_4$ and $ZnFe_2O_4$–Cu composites for excellent photocatalytic degradation of RhB dye', *Toxics*, vol. 12, no. 1, article 77, https://doi.org/10.3390/toxics12010077

Alzahrani, EA, Nabi, A, Kamli, MR, Albukhari, SM, Althabaiti, SA, Al-Harbi, SA, Khan, I & Malik, MA 2023, 'Facile green synthesis of ZnO NPs and plasmonic Ag-supported ZnO nanocomposite for photocatalytic degradation of methylene blue', *Water (Basel)*, vol. 15, no. 3, article 384, https://doi.org/10.3390/w15030384

Aouadi, A, Hamada Saud, D, Rebiai, A, Achouri, A, Benabdesselam, S, Mohamed Abd El-Mordy, F, Pohl, P, Ahmad, SF, Attia, SM, Abulkhair, HS, Ararem, A & Messaoudi, M 2024, 'Introducing the antibacterial and photocatalytic degradation potentials of biosynthesized chitosan, chitosan–ZnO, and chitosan–ZnO/PVP nanoparticles', *Scientific Reports*, vol. 14, no. 1, article 14753, https://doi.org/10.1038/s41598-024-65579-z

Basumatary, B, Atmanli, A, Azam, M, Basumatary, SF, Brahma, S, Das, B, Brahma, S, Rokhum, SL, Min, K, Selvaraj, M & Basumatary, S 2024, 'Catalytic efficacy, kinetic, and thermodynamic studies of biodiesel synthesis using *Musa* AAA plant waste-based renewable catalyst', *International Journal Energy Research.*, vol. 2024, pp. 1-27, https://doi.org/10.1155/2024/8837343

Bhatti, MA, Almani, KF, Shah, AA, Tahira, A, Chana, IA, Aftab, U, Ibupoto, MH, Mirjat, AN, Aboelmaaref, A, Nafady, A, Vigolo, B & Ibupoto, ZH 2022, 'Renewable and eco-friendly ZnO immobilized onto Dead Sea sponge floating materials with dual practical aspects for enhanced photocatalysis and disinfection applications', *Nanotechnology*, vol. 34, no. 3, article 035602, https://doi.org/10.1088/1361-6528/ac98cc

Edalati, K, Shakiba, A, Vahdati-Khaki, J & Zebarjad, SM 2016, 'Low-temperature hydrothermal synthesis of ZnO nanorods: Effects of zinc salt concentration, various solvents and alkaline mineralizers', *Materials Research Bulletin*, vol. 74, pp. 374–379, https://doi.org/10.1016/j.materresbull.2015.11.001

Fallahizadeh, S, Gholami, M, Rahimi, MR, Esrafili, A, Farzadkia, M & Kermani, M 2023, 'Enhanced photocatalytic degradation of amoxicillin using a spinning disc photocatalytic reactor (SDPR) with a novel Fe_3O_4@void@CuO/ZnO yolk-shell thin film nanostructure', *Scientific Reports*, vol. 13, no. 1, article 16185, https://doi.org/10.1038/s41598-023-43437-8

Fallahizadeh, S, Rahimi, MR, Gholami, M, Esrafili, A, Farzadkia, M & Kermani, M 2024, 'Novel nanostructure approach for antibiotic decomposition in a spinning disc photocatalytic reactor', *Scientific Reports*, vol. 14, no. 1, article 10566, https://doi.org/10.1038/s41598-024-61340-8

Ghasemi, Z, Younesi, H & Zinatizadeh, AA 2016, 'Kinetics and thermodynamics of photocatalytic degradation of organic pollutants in petroleum refinery wastewater over nano-TiO2 supported on Fe-ZSM-5', *Journal of the Taiwan Institute of Chemical Engineers*, vol. 65, pp. 357-366, https://doi.org/10.1016/j.jtice.2016.05.039

Hanh, NH, Nguyet, QTM, Van Chinh, T, Duong, LD, Tien, TX, Van Duy, L & Hoa, ND 2024, 'Enhanced photocatalytic efficiency of porous ZnO coral-like nanoplates for organic dye degradation', *RSC Advances*, vol. 14, no. 21, pp. 14672-14679, https://doi.org/10.1039/D4RA01345J

He, Z, Sun, C, Yang, S, Ding, Y, He, H & Wang, Z 2009, 'Photocatalytic degradation of Rhodamine B by Bi2WO6 with electron-accepting agent under microwave irradiation: Mechanism and pathway', *Journal of Hazardous Materials*, vol. 162, no. 2–3, pp. 1477–1486, https://doi.org/10.1016/j.jhazmat.2008.06.047

Hidayat, MI, Adlim, M, Suhartono, S, Hayati, Z & Bakar, NHH 2023, 'Antimicrobial air filter made of chitosan–ZnO nanoparticles immobilized on white silica gel beads', *Arabian Journal of Chemistry*, vol. 16, no. 8, article 104967, https://doi.org/10.1016/j.arabjc.2023.104967

Hidayat, MI, Adlim, M, Suhartono, S, Hayati, Z, Bakar, NHH, Ilham, Z & Hardiansyah, A 2024, 'Reusability and regeneration of antibacterial filter immobilized zinc oxide nanoparticles on white silica gel beads coated with chitosan', *South African Journal of Chemical Engineering*, vol. 50, pp. 200–208, https://doi.org/10.1016/j.sajce.2024.08.007

Hudaya, T, Kristianto, H & Meliana, C 2018, 'The simultaneous removal of cyanide and cadmium ions from electroplating wastewater using UV/TiO2 photocatalysis', *International Journal of Technology*, vol. 9, no. 5, pp. 964–971, https://doi.org/10.14716/ijtech.v9i5.1797

Humayoun, UB, Mehmood, F, Hassan, Y, Rasheed, A, Dastgeer, G, Anwar, A, Sarwar, N & Yoon, D 2023, 'Harnessing bio-immobilized ZnO/CNT/chitosan ternary composite fabric for enhanced photodegradation of a commercial reactive dye', *Molecules*, vol. 28, no. 18, article 6461, https://doi.org/10.3390/molecules28186461

Jesitha, K, Jaseela, C & Harikumar, PS 2018, 'Nanotechnology-enhanced phytoremediation and photocatalytic degradation techniques for remediation of soil pollutants', in *Nanomaterials for Soil Remediation*, pp. 463–499, https://doi.org/10.1016/B978-0-12-822891-3.00027-X

Joorabloo, A & Liu, T 2024, 'Recent advances in reactive oxygen species scavenging nanomaterials for wound healing', *Exploration*, vol. 4, no. 3, pp. 1–23, https://doi.org/10.1002/exp.20230066

Lal, M, Sharma, P, Singh, L & Ram, C 2023, 'Photocatalytic degradation of hazardous Rhodamine B dye using sol-gel mediated ultrasonic-hydrothermal synthesized ZnO nanoparticles', *Results in Engineering*, vol. 17, article 100890, https://doi.org/10.1016/j.rineng.2023.100890

Le, AT, Le, TDH, Cheong, K-Y & Pung, S-Y 2022, 'Immobilization of zinc oxide-based photocatalysts for organic pollutant degradation: A review', *Journal of Environmental Chemical Engineering*, vol. 10, no. 5, article 108505, https://doi.org/10.1016/j.jece.2022.108505

Li, Y, Lu, Q, Gamal El-Din, M & Zhang, X 2023, 'Immobilization of photocatalytic ZnO nanocaps on planar and curved surfaces for the photodegradation of organic contaminants in water', *ACS ES&T Water*, vol. 3, no. 8, pp. 2740–2752, https://doi.org/10.1021/acsestwater.3c00227

Look, DC 2001, 'Recent advances in ZnO materials and devices', *Materials Science and Engineering: B*, vol. 80, no. 1–3, pp. 383–387, https://doi.org/10.1016/S0921-5107(00)00604-8

Madani, H, Wibowo, A, Sasongko, D, Miyamoto, M, Uemiya, S & Budhi, YW 2024, 'Novel multiphase CO_2 photocatalysis system using N-TiO_2/CNCs and CO_2 nanobubble', *International Journal of Technology*, vol. 15, no. 2, pp. 432–441, https://doi.org/10.14716/ijtech.v15i2.6694

Medany, SS, Hefnawy, MA, Fadlallah, SA & El-Sherif, RM 2024, 'Zinc oxide–chitosan matrix for efficient electrochemical sensing of acetaminophen', *Chemical Papers*, vol. 78, no. 5, pp. 3049-3061, https://doi.org/10.1007/s11696-023-03292-3

Muktaridha, O, Adlim, M, Suhendrayatna, S & Ismail, I 2022, 'Highly reusable chitosan-stabilized Fe–ZnO immobilized onto fiberglass cloth and the photocatalytic degradation properties in batch and loop reactors', *Journal of the Saudi Chemical Society*, vol. 26, no. 3, article 101452, https://doi.org/10.1016/j.jscs.2022.101452

Muktaridha, O, Adlim, M, Suhendrayatna, S & Ismail, I 2023, 'Chemical component analysis of natural-rubber wastewater photocatalytic degradation', *Chemical Data Collections*, vol. 48, article 101057, https://doi.org/10.1016/j.cdc.2023.101057

Nafees, M, Liaqut, W, Ali, S & Shafique, MA 2013, 'Synthesis of ZnO/Al-doped ZnO nanomaterial: Structural and band gap variation in ZnO nanomaterial by Al doping', *Applied Nanoscience*, vol. 3, no. 1, pp. 49–55, https://doi.org/10.1007/s13204-012-0067-y

Natarajan, TS, Thomas, M, Natarajan, K, Bajaj, HC & Tayade, RJ 2011, 'Study on UV-LED/TiO2 process for degradation of Rhodamine B dye', *Chemical Engineering Journal*, vol. 169, no. 1–3, pp. 126–134, https://doi.org/10.1016/j.cej.2011.02.066

Nguyen, NT & Nguyen, VA 2020, 'Synthesis, characterization, and photocatalytic activity of ZnO nanomaterials prepared by a green, nonchemical route', *Journal of Nanomaterials*, vol. 2020, article 1768371, https://doi.org/10.1155/2020/1768371

Noman, MT, Amor, N, Petru, M, Mahmood, A & Kejzlar, P 2021, 'Photocatalytic behaviour of zinc oxide nanostructures on surface activation of polymeric fibres', *Polymers*, vol. 13, no. 8, article 1227, https://doi.org/10.3390/polym13081227

Ollis, DF 2018, 'Kinetics of photocatalyzed reactions: Five lessons learned', *Frontiers in Chemistry*, vol. 6, article 378, https://doi.org/10.3389/fchem.2018.00378

Piras, A, Olla, C, Reekmans, G, Kelchtermans, A-S, De Sloovere, D, Elen, K, Carbonaro, CM, Fusaro, L, Adriaensens, P, Hardy, A, Aprile, C & Van Bael, MK 2022, 'Photocatalytic performance of undoped and Al-doped ZnO nanoparticles in the degradation of Rhodamine B under UV–visible light: The role of defects and morphology', *International Journal of Molecular Sciences*, vol. 23, no. 24, article 15459 https://doi.org/10.3390/ijms232415459

Pompeu, LD, Muraro, PCL, Chuy, G, Vizzotto, BS, Pavoski, G, Espinosa, DCR, da Silva Fernandes, L & da Silva, W 2022, 'Adsorption for Rhodamine B dye and biological activity of nano-porous chitosan from shrimp shells', *Environmental Science and Pollution Research*, vol. 29, pp. 49858–49869, https://doi.org/10.1007/s11356-022-19259-y

Rajendrachari, S, Taslimi, P, Karaoglanli, AC, Uzun, O, Alp, E & Jayaprakash, GK 2021, 'Photocatalytic degradation of Rhodamine B (RhB) dye in wastewater and enzymatic inhibition study using cauliflower-shaped ZnO nanoparticles synthesized by a novel one-pot green synthesis method', *Arabian Journal of Chemistry*, vol. 14, no. 6, article 202106, https://doi.org/10.1016/j.arabjc.2021.103180

Sabatini, F, Giugliano, R & Degano, I 2018, 'Photo-oxidation processes of Rhodamine B: A chromatographic and mass spectrometric approach', *Microchemical Journal*, vol. 140, pp. 114–122, https://doi.org/10.1016/j.microc.2018.04.018

Sayem, MA, Hossen, SMA, Syed, IM & Bhuiyan, MA 2024, 'Effective adsorption and visible-light-driven enhanced photocatalytic degradation of Rhodamine B using ZnO nanoparticles immobilized on graphene oxide nanosheets', *Results in Physics*, vol. 58, article 107471, https://doi.org/10.1016/j.rinp.2024.107471

Sharfan, N, Shobri, A, Anindria, FA, Mauricio, R, Tafsili, MAB & Slamet 2018, 'Treatment of batik industry waste with a combination of electrocoagulation and photocatalysis', *International Journal of Technology*, vol. 9, no. 5, pp. 936–943, https://doi.org/10.14716/ijtech.v9i5.618

Silveira, MLDC, da Silva, NR, Padovini, DSS, Kinoshita, A, Pontes, FML & Magdalena, AG 2022, 'Synthesis, characterization, and photocatalytic activity of ZnO nanostructures', *Research, Society and Development*, vol. 11, no. 2, https://doi.org/10.33448/rsd-v11i2.25373

Sudol, E & Kozikowska, E 2021, 'Mechanical properties of polyurethane adhesive bonds in a mineral wool-based external thermal insulation composite system for timber frame buildings, *Materials,* vol. 14, no. 10, article 2527, https://doi.org/10.3390/ma14102527

Supin, KK, Namboothiri, PMP & Vasundhara, M 2023, 'Enhanced photocatalytic activity in ZnO nanoparticles developed using novel *Lepidagathis ananthapuramensis* leaf extract', *RSC Advances*, vol. 13, no. 3, pp. 1497–1515, https://doi.org/10.1039/D2RA06967A.

Thao, NT, Nga, HTP, Vo, NQ & Nguyen, HDK 2017, 'Advanced oxidation of Rhodamine B with hydrogen peroxide over ZnCr layered double hydroxide catalysts', *Journal of Science: Advanced Materials and Devices*, vol. 2, no. 3, pp. 317–325, https://doi.org/10.1016/j.jsamd.2017.07.005

Wahid, KA, Rahim, IA, Safri, SNA & Ariffin, AH 2023, 'Synthesis of ZnO nanorods at very low temperatures using ultrasonically pre-treated growth solution', *Processes*, vol. 11, no. 3, article 708, https://doi.org/10.3390/pr11030708

Wang, S, Jia, Y, Song, L & Zhang, H 2018, 'Decolorization and mineralization of Rhodamine B in aqueous solution with a triple system of cerium(IV)/H2O2/hydroxylamine', *ACS Omega*, vol. 3, no. 12, pp. 18456-18465, https://doi.org/10.1021/acsomega.8b02149

Yazdani, M, Virolainen, E, Conley, K & Vahala, R 2017, 'Chitosan–zinc(II) complexes as a bio-sorbent for the adsorptive abatement of phosphate: Mechanism of complexation and assessment of adsorption performance', *Polymers*, vol. 10, no. 1, article 25, https://doi.org/10.3390/polym10010025

Yudha, SS, Falahudin, A, Asdim & Han, JI 2020, 'Utilization of dammar gum as a soft template in titania synthesis for photocatalyst', *International Journal of Technology*, vol. 11, no. 4, pp. 842–851, https://doi.org/10.14716/ijtech.v11i4.4162

Zhang, T, Liu, Y, Wang, Y, Wang, Z, Liu, J & Gong, X 2023, 'Generation and transfer of long-lifetime reactive oxygen species (ROS) from electrochemical regulation', *Chemical Engineering Journal*, vol. 464, article 142443, https://doi.org/10.1016/j.cej.2023.142443